Journal of Medicinal Chemistry

Article

pubs.acs.org/jmc

High-Throughput Virtual Screening Identifies Novel *N*′-(1-Phenylethylidene)-benzohydrazides as Potent, Specific, and Reversible LSD1 Inhibitors

Venkataswamy Sorna,[†,⊥] Emily R. Theisen,[†,‡,⊥] Bret Stephens,[†] Steven L. Warner,[†] David J. Bearss,[†] Hariprasad Vankayalapati,[†,§] and Sunil Sharma*[,†,§,∥]

[†]Center for Investigational Therapeutics (CIT), Huntsman Cancer Institute, University of Utah, 2000 Circle of Hope, Salt Lake City, Utah 84112, United States

[‡]Department of Pharmaceutics and Pharmaceutical Chemistry, College of Pharmacy, University of Utah, 301 Skaggs Hall, Salt Lake City, Utah 84112, United States

[§]School of Medicine, University of Utah, 30 North 1900 East, Salt Lake City, Utah 84132, United States

[∥]Division of Medical Oncology, Huntsman Cancer Institute, University of Utah, 2000 Circle of Hope, Salt Lake City, Utah 84112, United States

Supporting Information

ABSTRACT: Lysine specific demethylase 1 (LSD1) plays an important role in regulating histone lysine methylation at residues K4 and K9 on histone H3 and is an attractive therapeutic target in multiple malignancies. Here we report a structure-based virtual screen of a compound library containing ∼2 million small molecular entities. Computational docking and scoring followed by biochemical screening led to the identification of a novel *N*′-(1-phenylethylidene)-benzohydrazide series of LSD1 inhibitors with hits showing biochemical IC_{50}s in the 200−400 nM range. Hit-to-lead optimization and structure−activity relationship studies aided in the discovery of compound **12**, with a K_i of 31 nM. Compound **12** is reversible and specific for LSD1 as compared to the monoamine oxidases shows minimal inhibition of CYPs and hERG and inhibits proliferation and survival in several cancer cell lines, including breast and colorectal cancer. Compound **12** may be used to probe LSD1's biological role in these cancers.

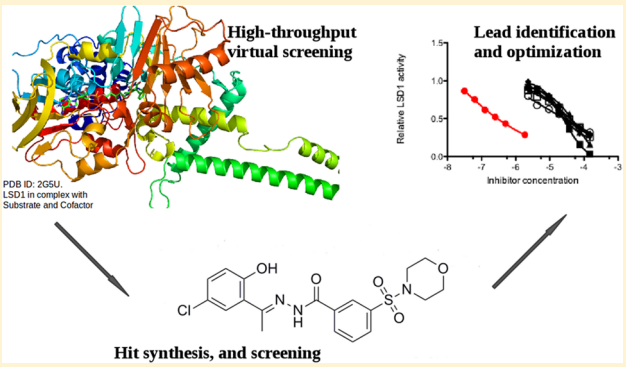

1. INTRODUCTION

Epigenetic disregulation contributes to the aberrant gene expression programs characteristic of cancer.[1,2] Transcriptional regulation through chromatin modification is reversible and dynamic such that enzymes implicated in the disregulation of chromatin represent a new class of protein targets for drug development. Various chromatin modifications mediate changes in gene expression including DNA methylation, posttranslational histone modifications, and nucleosome remodeling. The N-terminal tails of histones are subject to a variety of posttranslational modifications such as phosphorylation, acetylation, methylation, and ubiquitination. Certain modifications, particularly lysine acetylation and methylation, are important for regulating the local chromatin state and are often disregulated in cancer.[2]

Histone methylation was believed to be an irreversible mark until the discovery of lysine-specific demethylase 1 (LSD1) in 2004.[3] LSD1 catalyzes the oxidative demethylation of mono- and dimethylated histone H3 at lysine 4 (H3K4me1 and H3K4me2) and lysine 9 (H3K9me1 and H3K9me2) through a flavin adenine dinucleotide (FAD)-dependent amine oxidase reaction.[3,4] While histone acetylation is associated with open chromatin and gene activation, the impact of histone methylation on the local chromatin state is more nuanced.[5] Using the substrates for LSD1 as an example, H3K4 methylation is generally associated with gene activation, whereas methylation of H3K9 is associated with transcriptional repression.[6] In this manner, LSD1 can act either as a corepressor or coactivator depending on its substrate.[7,8] Thus, LSD1 is a component of both repressive and activating complexes and the substrate specificity of LSD1 depends on which complex LSD1 interacts with. Repressive complexes containing histone deacetylases (HDACs), CtBP, CoREST, and BHC80 target LSD1 toward H3K4.[9−12] In these complexes, HDACs remove the H3K9 acetyl mark, allowing LSD1 access to H3K4 methylation.[13,14] The unmethylated histone tail will then be bound by BCH80 to maintain the

Received: June 12, 2013
Published: November 17, 2013

repressive state.[11] However, in complex with the estrogen or androgen receptor, LSD1 is targeted toward H3K9 at the promoters of target genes.[4,10,15] Subsequent demethylation of H3K9 results in the activation of estrogen and androgen receptor target genes.[4,16]

LSD1 is a therapeutic target in cancer with overexpression observed in a variety of solid tumors, including neuroblastoma, breast, prostate, bladder, lung, liver, and colorectal tumors.[16−20] In many of these cases, LSD1 is reported as a corepressor with specificity for H3K4. Increased methylation at the H3K4 mark through either LSD1 knockdown or inhibition was shown to reactivate expression of tumor suppressor genes in breast, bladder, lung, and colorectal cancers.[18,21] In hormone-responsive cancer, association of LSD1 with the estrogen and androgen receptors led to increased proliferation.[4,15] LSD1 inhibition decreased expression of target genes in these models. Thus, inhibition of LSD1 is an effective strategy to reexpress epigenetically silenced tumor suppressor genes as well as downregulate important proliferative pathways in multiple cancer types. However, because of the complexity of factors regulating LSD1 function, the precise role LSD1 plays in cancer and how that role differs between cancers is not fully understood.

Several LSD1 inhibitors are reported (Chart 1), but they show poor selectivity and pharmacological properties making further exploration of LSD1 biology difficult. Monoamine oxidase (MAO) inhibitors such as tranylcypromine (TCP) and pargyline are known irreversible LSD1 inhibitors (**A** and **B**), and several reported inhibitors (**C**−**L**)[22−29] are derivatives of these scaffolds with increased selectivity for LSD1. Peptide derivatives of pargyline have also been investigated, but delivery of peptide therapeutics to the nucleus remains an unsolved issue.[30,31] Polyamine derivatives were also evaluated as LSD1 inhibitors (**M** and **N**), with compounds showing biochemical activity in the low micromolar range.[21,32,33] Other reversible LSD1 inhibitors are reported to show selective activity against stem-like cancer cells (**O**)[34] and castration-resistant prostate cancer (**P**).[35] In vivo efficacy is reported for the reversible inhibitor, namoline (**P**), however this was accompanied by significant weight loss indicative of off-target toxicity.[35] In general, currently available small molecule LSD1 inhibitors display poor selectivity, low potency, or in vivo toxicity, limiting further interrogation of LSD1's contribution to cancer at the organismal level. Identification of novel potent, selective, and reversible LSD1 inhibitors is essential to further elucidate LSD1's role in cancer and identify whether or not reversible inhibition targeting LSD1 is a viable therapeutic strategy.

Here, we report a structure-based virtual screen (VS) of a diverse compound library utilizing docking with Glide, ICM, GOLD scoring, and GOLD consensus rescoring energy calculations, which led to the identification of a novel *N*′-(1-phenylethylidene)-benzohydrazide series of LSD1 inhibitors. On the basis of the initial hits, we rationally designed a series of small molecule LSD1 inhibitors which resulted in a selective and potent lead compound **12** which is a reversible and noncompetitive LSD1 inhibitor.

Chart 1. Representative Structures of Reported Classes of LSD1 Inhibitors[a]

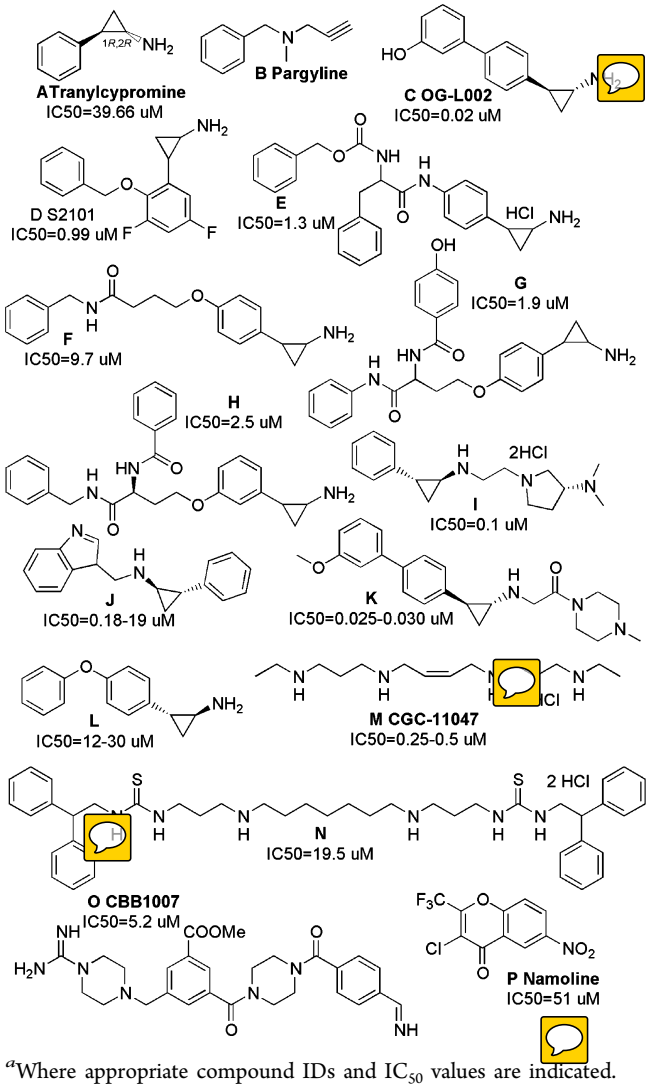

[a]Where appropriate compound IDs and IC_{50} values are indicated.

2. RESULTS

2.1. Docking Studies. The docking protocols used by both ICM and Glide SP were run with the adenosine phospate fragment of FAD, riboflavin fragment of FAD, and known LSD1 ligands from Chart 1 as positive controls within the Glide dl-400 1000-compound decoy set to confirm the accuracy of the docking protocols. Specifically, known LSD1 ligands were identified in the top 2% of the total decoy set. The structure-based VS was performed using the Glide docking module within the Schrödinger Suite 2011. The small molecule ligand library of 13 million compounds was first docked using Glide High Throughput Virtual Screen (HTVS), a method specifically proven to discard noticeable nonbinders with minimal computational time and then filtered for standard rule-of-five (RO5) criteria, medchem tractability based on physicochemical parameters in predicted in QikProp, and undesireable chemical features. The top 15% of compounds (∼2 million) from HTVS were then redocked with the more computationally expensive Glide standard precision (SP) scoring. This led to the selection of 0.5% (∼10000) of the top-ranked compounds by SP for subsequent screening using Glide extra-precision (XP) and ICM docking and scoring methods. These methods from the Schrödinger and Molsoft suites, respectively, are more resource intensive and used in our workflow to minimize false positives.

While molecular docking has proven a useful tool to quickly identify bioactive compounds, there are still problems with the accuracy and consistency of scoring functions in VS methods.

dx.doi.org/10.1021/jm400870h | J. Med. Chem. 2013, 56, 9496−9508

Hence, we identified 121 compounds which scored either < −5.0 kcal/mol using Glide SP/XP or < −15.0 kcal/mol using ICM in addition to meeting certain physicochemical criteria, including solubility >50 μg/mL, permeability >50 nmol/s, and polar surface area (PSA) <120 Å^2 as determined by QikProp. In addition to the algorithm rankings, redundant compounds were removed to improve chemical diversity of the final selections and visual inspection of the docking results was used to evaluate binding mode, position, and orientation. Taken together, this methodology identified a set of 121 hits for further analysis. GOLD was used to rescore these hits. The GOLD consensus scoring and fitness functions produced similar compound rankings within the 121 hits to that of ICM and Glide scores, further supporting our hit selection process. Interestingly, compounds with hydroxyl moieties, hydrophobic electron withdrawing groups, and heterocycloalkyl groups were well represented in the initial docking experiments from all VS programs used.

2.2. Initial Hits. On the basis of the selection criteria discussed above, 121 structurally distinct compounds were procured and screened in the LSD1 biochemical assay. This identified a series of *N*′-(1-phenylethylidene)-benzohydrazides, which showed potent activity against LSD1. Biochemical assay results and docking scores for the series are reported in Table 1, Supporting Information Tables S1 and S2. Out of the 121 in silico hits tested for LSD1 activity, compounds **1**−**5** showed biochemical activity in the 200−400 nM range. Compound **6** showed an IC_{50} of 19 nM against LSD1. The docking poses determined from all three programs were predicted to be similar and show the protonated morpholin ring nitrogen of compound **6**, forming a favorable ionic interaction. Interestingly, the 2-hydroxyphenyl moiety of compound **6** extended deeper into the pocket as compared to compounds **1**−**5**. A representative binding mode is shown in Figure 1. These initial hits support the utility of our VS methodology. Compounds **7**−**10** had similar core structures to compounds **1**−**6** and represented some of the chemical diversity present in the 121 hits. These compounds included substitution of the critical 2-hydroxylphenyl groups with biaryl naphthalene (**7**), an electron donating methoxyl group (**8**), absence of the hydroxyl group (**9**), and the introduction of a small hydrophobic methyl group with a lack of 2-hydroxyl (**10**). The additional 111 negative hits are reported in Supporting Information Table S2.

Table 1. Commercially Available Highly-Ranked Hits from 121 Screened Compounds[a]

S. No	Structure	IC_{50} (μM) LSD1
1	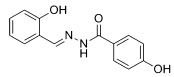	0.218
2	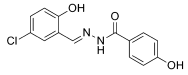	0.275
3	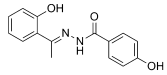	0.291
4	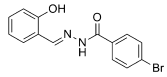	0.196
5	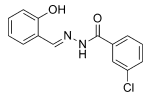	0.333
6	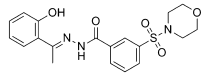	0.019
7	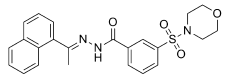	>10
8	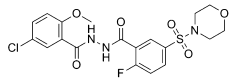	>3
9	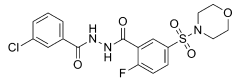	>3
10	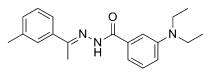	>3

[a]Included are biochemical IC_{50}s for compound **1**−**10**.

The biochemical data showed compounds having 4-OH, 4-Br, or 3-Cl aryl substitutions on the benzohydrazides (compounds **1**, **4**, and **5**, respectively) had similar activity against LSD1 with IC_{50}s of 218, 196 nM, and 333 nM, respectively. The 5-chloro-2-hydroxyl substituted derivative (**2**) and *N*′-(1-phenylethylidene)-benzohydrazide core (**3**) are well tolerated, with IC_{50}s of 275 and 291 nM, respectively. The 3-substituted sulfonyl functional group on the arylhydrazide moiety of compound **6** improved biochemical activity10-fold with an IC_{50} of 19 nM. The exchange of the 2-hydroxyphenyl moiety with naphthalene in compound **7** impaired biochemical activity with an IC_{50} > 10 μM. Compounds **8**−**10** were representative examples of the remaining negative hits and showed no biochemical activity in the LSD1 assay. These biochemical results suggested further optimization of compounds **1**−**6** to explore the structure−activity relationship of the *N*′-(1-phenylethylidene)-benzohydrazide series and identified potential lead compounds shown in Table 2 for further screening against LSD1.

2.3. Structure−Activity Relationship of Initial Hits and Compound Optimization. Compounds **11**−**22** were subsequently synthesized in-house, and their chemical structures and LSD1 inhibition are reported in Table 2. We utilized the *N*′-(1-phenylethylidene)benzohydrazide core scaffolds from hit compounds **3** and **6** for further optimization and SAR in order to increase metabolic stability over the benzylidenebenzohydrazide core of compounds **1**, **2**, **4**, and **5**. In compound **11**, removing the sulfonyl moiety and retaining the 5-chloro-2-hydroxyphenyl group from compound **2** maintained a biochemically active compound (IC_{50} = 128 nM) with a 10-fold reduction in potency as compared to **6**. In the case of **12**, reintroduction of the sulfonyl functional group and inclusion of the 5-chloro-2-hydroxyphenyl moiety on the *N*′-(1-phenylethylidene)benzohydrazide inhibited LSD1 with an IC_{50} of 13 nM, which is comparable to compound **6**. A representative binding mode of **12** generated from ICM is shown in Figure 1. Exchanging 2-hydroxyl with 2-chloro in compound **13** resulted in a complete loss of LSD1 activity, emphasizing the importance of the 2-hydroxyl group. As shown in Figure 1, the 2-hydroxyl moiety participates in hydrogen bonding and loss of this interaction likely impairs ligand binding. Replacement of the morpholin with an *N*,*N*-dimethyl sulfonamide (**14**) maintained LSD1 potency with an IC_{50} of 14 nM, highlighting the significance of the core sulfonamide. On the basis of Figure 1, we hypothesized both *N*′-(1-phenylethylidene)benzohydrazide and *N*′-(1-phenylpropylidene)benzohydrazide were likely accommodated, however the *N*′-(1-phenylpropylidene)benzohydrazide deriva-

dx.doi.org/10.1021/jm400870h | J. Med. Chem. 2013, 56, 9496−9508

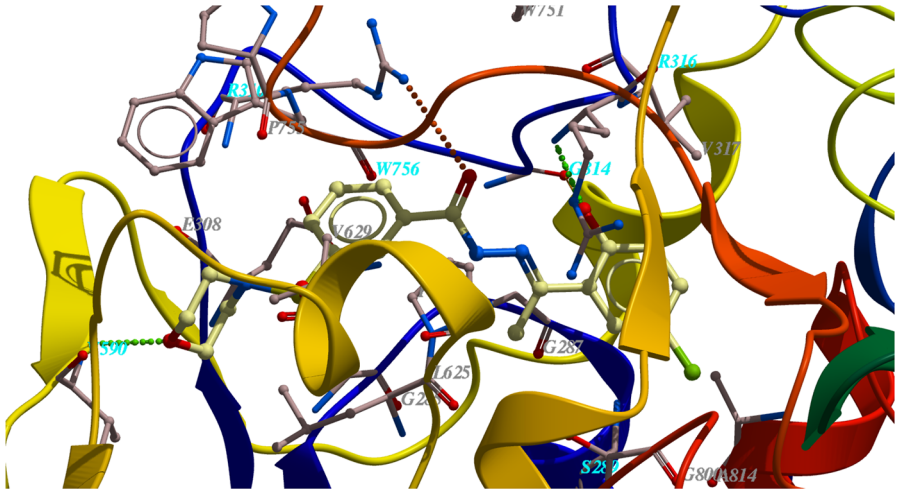

Figure 1. Mode of binding of compound **12** in complex with LSD1. The H-bonding interactions of compound **12** with LSD1 are depicted in dashed lines.

Table 2. Synthesized Compounds and Their Biochemical Activity against LSD1

S. No	Structure	IC_{50} (μM) LSD1
11	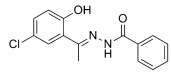	0.128
12	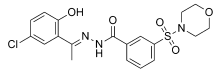	0.013
13	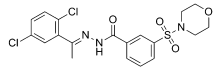	>3
14	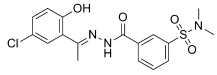	0.014
15	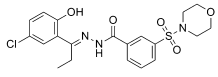	>3
16	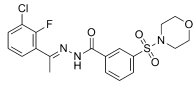	>3
17	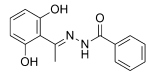	>3
18	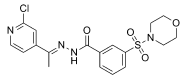	>3
19	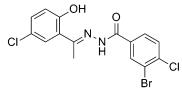	>3
20	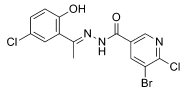	>3
21	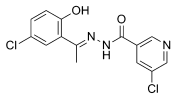	>3
22	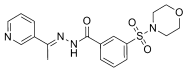	>3

tive (**15**) showed no LSD1 activity (IC_{50} > 3 μM). Generally, compounds **15**–**22** showed no activity against LSD1 in the biochemical assay. An additional polar hydroxyl group did not improve LSD1 activity nor did disubstitution of the aryl ring with strong electron withdrawing groups, like −F. Further, introduction of various heterorings were not tolerated. Because of the favorable biochemical activity of compound **12**, we utilized it to further investigate the mechanism of inhibition of this series of LSD1 inhibitors.

2.4. Scaffold Novelty. Many different classes of LSD1 inhibitors are already reported (Chart 1), with some compounds showing nanomolar potency. We wanted to evaluate the similarity of the *N*′-(1-phenylethylidene)-benzohydrazide scaffold to previously reported inhibitors. The calculated Tanimoto similarity coefficients are reported in Supporting Information Table S3. Typically, 0.7 is used as a cutoff, with >0.7 indicating similar compounds. Generally, the similarity coefficients calculated are all <0.4, ranging from 0.11 to 0.39, demonstrating that compound **12** is structurally distinct from previously reported LSD1 inhibitors. The most dissimilar compounds were the polyamine derivatives (**M** and **N**) and the reversible inhibitor namoline (**P**), with similarity scores of 0.11. The most similar compounds were various derivatives of tranylcypromine (**F**, **J**, and **K**), with similarity scores of 0.35, 0.36, and 0.39, respectively. The similarity score for the other reversible inhibitor reported, **O**, was calculated to be 0.32. These results corroborated the novelty of the *N*′-(1-phenylethylidene)-benzohydrazide series, represented in Tables 1 and 2.[36]

2.5. Lead Compound 12 Is Specific and Reversible. The specificity of the compounds **1** and **12** were tested in MAO A and MAO B biochemical assays (Figure 2). In this assay, the MAO inhibitor TCP exhibited activity against both MAO A and B, with an IC_{50} of 2.1 and 3.6 μM, respectively. Compound **1** was active against MAO B, with an IC_{50} of 1.3 μM, but showed no activity against MAO A (IC_{50} > 300 μM). In contrast, compound **12** did not exhibit activity against either MAO enzyme up to 300 μM. We further screened **12** against D-lactate dehydrogenase, glucose oxidase, a panel of cytochrome P450s (CYP), and human ether-à-go-go (hERG), with IC_{50} values summarized in Table 3. Using an IC_{50} of 3 μM as a cutoff, **12** showed low activity against CYP3A4, with an IC_{50} of 2.96 μM. The inhibition data for the off-target assays are reported in the Supporting Information (Table S4).

We performed a jump dilution to assay the reversibility of compound **12** (Figure 3). In this assay, LSD1 was incubated

dx.doi.org/10.1021/jm400870h | J. Med. Chem. 2013, 56, 9496−9508

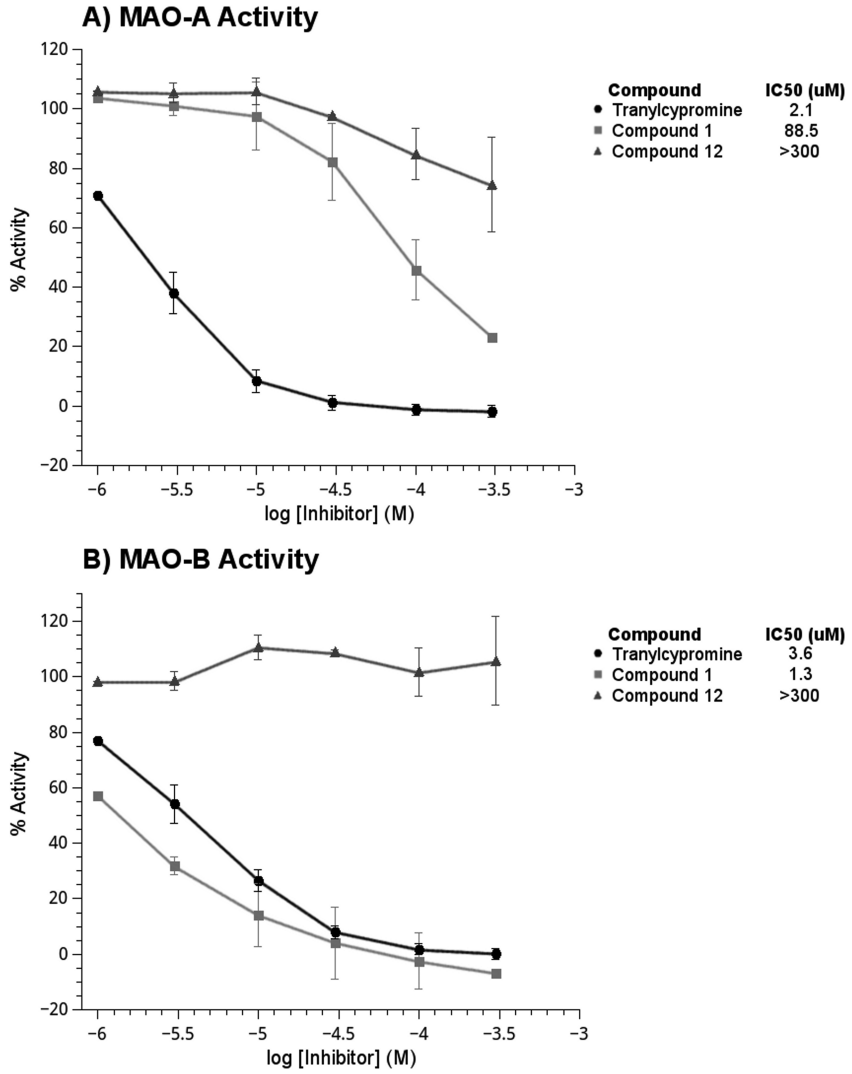

Figure 2. MAO activity of select compounds. (A) The MAO inhibitor TCP inhibited MAO A with an IC_{50} of 2.1 μM, while compounds **1** and **12** inhibited MAO A with IC_{50}s of 88 and >300 μM, respectively. (B) Compound **12** did not inhibit MAO B at the concentrations tested (IC_{50} > 300 μM). However, compound **1** exhibited significant activity against MAO B, with an IC_{50} of 1.3 μM, similar 3.6 μM for TCP.

Table 3. Off-Target Panel for Compound 12

enzyme	IC_{50} (μM)
D-lactate dehydrogenase	>10
glucose oxidase	>10
CYP1A2	>10
CYP2C19	9.76
CYP2C9	8.04
CYP2D6	>10
CYP3A4	2.61
hERG	>10

with 10× the biochemical IC_{50} of **12** for 1 h and then diluted 100-fold into the assay. The irreversible inhibitor TCP was used as a positive control, and the chemically similar but inactive compound **13** was used as a negative control. TCP incubation resulted in complete inactivation of the enzyme, which was not recovered once diluted into the assay buffer. When LSD1 was diluted into assay buffer after incubation with compound **12**, its activity returned with only 14.4 ± 3% inhibition. When the drug concentration was held constant at 200 nM through the dilution, activity was inhibited 65.7 ± 5%, suggesting

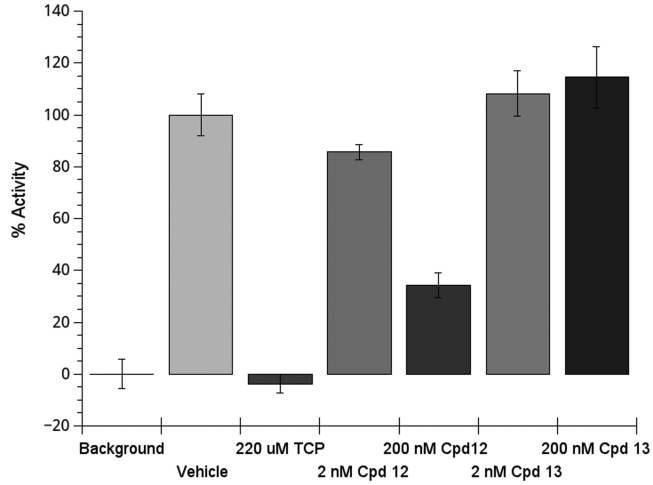

Figure 3. Compound **12** reversibly inhibits the activity of LSD1. Dilution of compound **12**, but not of the covalently binding inhibitor TCP, results in recovery of LSD1 activity. Compound **13** is inactive.

dx.doi.org/10.1021/jm400870h | J. Med. Chem. 2013, 56, 9496−9508

compound **12** is a reversible inhibitor. Compound **13** showed no activity in this assay.

2.6. Compound 12 Is a Noncompetitive Inhibitor. We further performed differential scanning fluorimetry (DSF) to compare the melting profile of LSD1 bound by compound **12** with the LSD1-TCP complex. DSF uses SYPRO Orange, which preferentially fluoresces in the amphiphilic molten globule state of an unfolding protein. LSD1 was incubated either with compound **12**, **13**, or TCP for 30 min, and then DSF was performed. The raw melt curves were smoothed and fit to a Boltzmann curve for unfolding using Applied Biosystem's Protein Thermal Shift (PTS) software. Derivatives of the smoothed curves were plotted to generate the derivative plot shown in Figure 4. Both Boltzmann and derivative melting

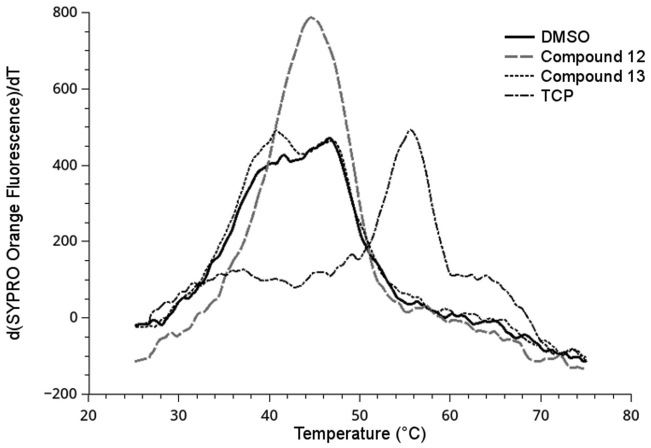

Figure 4. Derivative melt curves of LSD1 in the presence of DMSO, compound **12**, compound **13**, and TCP. LSD1 has a complex multiphase melt. Compound **12** and TCP induce changes in LSD1's melt profile in distinct manners. Compound **13** shows no difference from DMSO.

temperatures (T_m) were determined for each condition and are shown in Table 4. LSD1 alone showed a multiple-phase

Table 4. Melting Temperatures as Determined by DSF

treatment	Boltzmann T_m ± SD (°C)	first derivative T_m ± SD (°C)	second derivative T_m ± SD (°C)
DMSO	43.28 ± 0.45	40.49 ± 0.81	46.31 ± 1.08
15 μM **12**	44.60 ± 0.47	45.35 ± 1.27	N/A
15 μM **13**	43.29 ± 0.67	40.76 ± 0.58	46.69 ± 0.76
220 μM TCP	51.98 ± 1.18	55.60 ± 0.32	N/A

unfolding with a Boltzmann T_m of 43.28 ± 0.45 °C and derivative T_ms at 40.49 ± 0.81 °C and 46.31 ± 1.1 °C. Compound **13** exhibited no effect on LSD1.

TCP stabilized LSD1 with a clear rightward shift of the derivative curve. Additional inspection of the data showed a long period of slow melting, followed by a sharp transition between 50 and 60 °C. The Boltzmann T_m was determined as 51.98 ± 1.2 °C, and the derivative method placed the T_m during the rapid melt phase at 55.60 ± 0.32 °C. Compound **12** shifted the T_m in a subtle but statistically significant fashion and constrained the melting dynamics of LSD1 to classical two-state unfolding. The Boltzmann T_m for compound **12** was 44.60 ± 0.47 °C with a derivative T_m of 45.38 ± 1.3 °C. This suggests compound **12** binds LSD1, changes its solution dynamics in a manner distinct from TCP, and shows small change in T_m.

We used enzyme kinetics to investigate the mechanism of action of compound **12**. For each drug concentration, the initial velocity of the biochemical assay was plotted with respect to enzyme substrate in Figure 5. Our calculated K_m of 1.3 ± 0.2

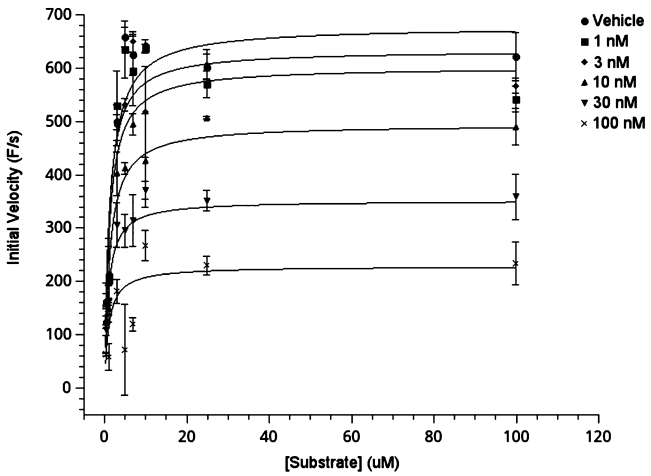

Figure 5. LSD1 kinetics with multiple concentrations of compound **12**. Compound **12** causes a decrease in v_{max} with no change in K_m, characteristic of noncompetitive inhibition.

μM is similar to previous literature reports for the dimethylated K4 N-terminal H3 peptide.[14] Curves were analyzed individually using the Michaelis–Menten suite or globally using the Enzyme Inhibition suite in GraphPad Prism 5, with the results of the analysis summarized in Table 5. The global fit to a mixed model inhibition gave a K_i of 31 ± 12 nM and an α value of 1.3, which is most indicative of noncompetitive inhibition. This is consistent with the observed drop in v_{max} and little change in K_m with increasing concentration of **12**. (For a comparison of competitive, noncompetitive, and uncompetitive inhibition global curve fits, see Supporting Information Table S5.) Individually fitting each curve and using this data to determine a K_i for compound **12** produced a K_i of 34 ± 1.9 nM, which correlated well with the global fit.

2.7. Compound 12 Activity in in Vitro Assays. Compound **12** was used to evaluate sensitivity in a panel of cancer cell lines (Table 6). Cell line sensitivity to compound **12** varied by one log in a cell viability assay, with EC_{50} values ranging from 300 nM to 3 μM. Nine of the 17 cell lines tested were sensitive to compound **12**, with an EC_{50} < 1 μM. Endometrial, breast, colorectal, and pancreatic cancers were represented in the sensitive lines, consistent with a role for LSD1 in multiple cancers. EC_{50} values were determined in T-47D breast cancer cells to evaluate the correlation between cell sensitivity and biochemical activity against LSD1 (Table 7). With few exceptions, it was observed that T-47D cells were sensitive to test compounds that were active in the LSD1 biochemical assay. For compounds inactive in the biochemical assay, cellular sensitivity was more variable (Figure 6). Compounds with low EC_{50}s against T-47D cells but no biochemical activity may possess uncharacterized cytotoxic off-target activity. The only active biochemical compounds without T-47D activity were compounds **1** and **14**. These compounds may show decreased permeability or solubility in the cell-based assay format, although compound **14** still shows activity near

dx.doi.org/10.1021/jm400870h | J. Med. Chem. 2013, 56, 9496–9508

Table 5. Summary of Michaelis–Menten Curve Fits

fit	v_{max} (F/s) ± std error	K_m (μM) ± std error	k_i (nM) ± std error	α ± std error	R^2
global: mixed Model Inhibition	687 ± 11.43	1.284 ± 0.1048	30.69 ± 12.4	1.333 ± 0.64	0.9241
DMSO	697.5 ± 26.32	1.405 ± 0.2514	N/A	N/A	0.9275
1 nM	649.4 ± 30.09	1.140 ± 0.2662	13.50	N/A	0.8807
3 nM	642.9 ± 27.07	1.393 ± 0.2787	35.32	N/A	0.9082
10 nM	531.1 ± 19.53	1.508 ± 0.2573	31.92	N/A	0.9308
30 nM	376.4 ± 12.25	1.108 ± 0.1832	35.17	N/A	0.9326
100 nM	246.5 ± 19.57	2.267 ± 0.7461	54.66	N/A	0.7803
average k_i	N/A	N/A	34.11 ± 6.54	N/A	N/A

Table 6. Compound 12 Inhibits Proliferation in Several Cell Lines in Vitro

cell line	IC_{50} (μM)	cancer type
AN3 Ca	0.356	endometrial
BT-20	0.489	breast
BT-549	1.010	breast
HCT 116	0.614	colorectal
HER218	0.612	breast
Hs-578-T	1.700	breast
HT29	0.429	colorectal
MCF-7	0.637	breast
MDA-MB-231	1.040	breast
MDA-MB-435	1.440	melanoma
MDA-MB-468	2.730	breast
MIA PaCa-2	0.468	pancreatic
PANC-1	1.104	pancreatic
PC-3	2.160	prostate
SK-N-MC	0.329	sarcoma
T-47D	0.649	breast
U87	1.160	glioblastoma

Table 7. In Vitro Growth Inhibition of Compound Panel in T-47D Cells

compound	IC_{50} (μM)
1	2.700
2	0.821
3	0.971
4	0.096
5	0.615
6	0.524
7	>10
8	>10
9	>10
10	>10
11	0.352
12	0.649
13	1.700
14	1.375
15	0.352
16	>10
17	>10
18	>10
19	0.565
20	0.270
21	0.616

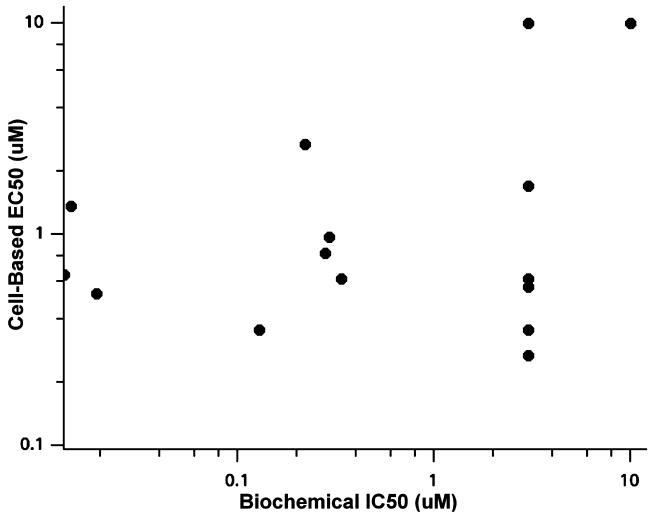

Figure 6. Compounds with biochemical activity against LSD1 show in vitro EC_{50}s clustered near 1 μM. Compounds without LSD1 activity show a wide range of in vitro efficacy.

1 μM. Importantly, when the hydroxyl of compound **12** was substituted with a chlorine (compound **13**), in vitro activity was lost, confirming the importance of the hydroxyl group in that position for both biochemical and cellular activity.

In addition to cell viability, we assayed compound **12** for its effect on histone methylation in an androgen-sensitive prostate cancer cell line, VCaP. VCaP cells were treated for 24 h with vehicle or 0.1, 1, or 10 μM of compound **12** for 24 h. We focused specifically on the H3K9me2 mark. H3K9me2 is a target for LSD1 in complex with the androgen receptor in prostate cancer.[4,15] Demethylation of this mark activates transcription of androgen receptor target genes.[4,15] An increase in H3K9me2 is observed at 24 h with both 1 and 10 μM of treatment with **12** (Figure 7). This suggests the antiproliferative effects of compound **12** are on-target and related to changes in histone methylation mediated through reversible LSD1 inhibition.

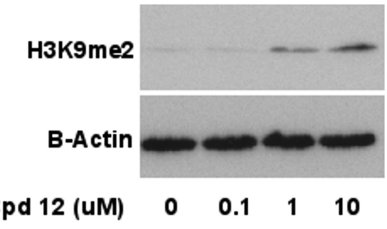

Figure 7. VCaP cells treated with compound **12** show a dose-dependent increase in H3K9 dimethylation.

dx.doi.org/10.1021/jm400870h | J. Med. Chem. 2013, 56, 9496–9508

3. DISCUSSION

We used a virtual screen (VS) methodology with a custom compound library to evaluate the chemical space outside of previously reported LSD1 inhibitors. All computational methods utilized the crystal structure of LSD1 in complex with an FAD-tranylcypromine adduct (PDB ID: 2Z5U).[37] The virtual small molecule screening library was curated from publicly available vendor libraries, totaling ∼13 million compounds. We then performed structure-based VS using Glide in HTVS mode to weed out noticeable nonbinders along with custom filters to narrow the library to ∼2 million compounds having drug-like properties and chemical diversity. Filters included medchem tractability, based on physicochemical parameters calculated in QikProp, and undesirable chemical features in addition to rule-of-five-based parameters (<5 H-bond donors, <8 H-bond acceptors, CLogP < 5, and molecular weight <500). This custom protocol increases the probability that hits from the top 0.5% of compounds from subsequent Glide SP docking will display favorable properties for later lead optimization and lead compound development. By cross-comparing results from three different docking algorithms (ICM, Glide XP, and GOLD), this study identified 121 initial hits that were procured and screened against LSD1 in a biochemical assay. Twelve novel compounds were subsequently synthesized in-house based on the SAR of the initial positive hits (**1**−**6**) to further elucidate the SAR, optimize drug-like properties, and increase potency. Biochemical activity for compounds **1**−**21** correlated well with in vitro activity in a breast cancer cell line, T-47D. Generally, compounds which were active in the biochemical assay showed an EC_{50} in T-47Ds near or below 1 μM, suggesting a similar and consistent mechanism of action. Compounds with poor biochemical activity showed a range of activity in the cell viability assay, which indicates some of the compounds inactive against LSD1 may have uncharacterized off-target toxicities in vitro.

Ultimately, our lead optimization strategy successfully identified a series of compounds more potent and specific than other reported LSD1 inhibitors. Tanimoto similarity scores are reported (Supporting Information Table S3) comparing compound **12** against previously reported LSD1 inhibitors. The low range of similarity scores (0.11−0.39) supports these compounds as a novel class of LSD1 inhibitors. The in-house-synthesized compounds **11**, **12**, and **14** showed biochemical IC_{50}s between ∼10 and 300 nM against LSD1 compared to 39.7 μM for TCP, which forms a noncovalent adduct with the FAD. The novelty of the scaffold may contribute to the improved specificity profile against the MAOs after lead optimization as compared to those reported for other compounds.[22] FAD is bound in LSD1 by a Rossman fold in a manner homologous to MAO A and B. Given the high structural homology of LSD1 to the monoamine oxidase family of enzymes (17.6% for both MAO A and B),[38] these are likely off-target hits for LSD1 inhibitors. TCP and pargyline derivatives targeting the H3-binding cavity of LSD1 often show some activity against either MAO A or MAO B, limiting their use in preclinical studies. Optimization from compound **1** to compound **12** improved the specificity profile where the initial hit compound **1** was more active against the MAO B and compound **12** displayed a favorable off-target profile with minimal activity against both MAO A and B. Compound **12** was also selective over other flavoenzymes D-LDH and GO as well as against cytochrome P450s and hERG.

We predicted that our lead optimization strategy would select reversible inhibitors of LSD1. Subsequent jump dilution experiments confirmed the reversibility of compound **12**, inactivity of compound **13**, and the irreversible mechanism of action of TCP. DSF analysis was performed to further probe the physical effect of compound **12** as compared to irreversible inhibition. In these experiments, LSD1 alone and in the presence of **13** shows a multiphase melting curve (Figure 4). This may indicate either two domains which melt at different temperatures or two populations of conformers with different thermal stability. The addition of compound **12** shows subtle changes in the T_m, with an effect on the melt profile evident in the derivative curve. Here, compound **12** appears to constrain LSD1's derivative profile to a Boltzmann distribution indicative of a classical two-state unfolding. Irreversible inhibition with TCP shows a long period of slow "melting" followed by a sharp melt between 50 and 60 °C. We conclude compound **12** alters the solution dynamics of LSD1 in a manner distinct from TCP.

Kinetic analysis was used to elucidate the reversible mechanism of action of our inhibitor series and to determine a K_i for compound **12**. Michaelis−Menten plots were generated across five inhibitor concentrations and seven substrate concentrations. A global fit of the data showed that non-competitive inhibition best described compound **12**'s mechanism of action. This is corroborated by the decreased v_{max} and unchanged K_m observed when the individual curves for each inhibitor are fit independently. The K_i of **12** was near 30 nM. Compound **12** does not interfere with the binding of the N-terminal H3 peptide so transcription factors with N-terminal sequences homologous to histone H3 that have been shown to recruit LSD1, such as SNAI1 and Gfi-1, may still be able to recruit an inactive LSD1 via their SNAG domains.[39−41] However, if the conformational dynamics of LSD1 are constrained by compound **12**, other key protein−protein interactions which regulate LSD1's activity may be disrupted. Further studies are required to determine the effect of compound **12** on the protein−protein interactions which guide LSD1's biological function.

Compound **12** shows cellular activity against several cancer cell lines including endometrial, breast, colorectal, pancreatic, and prostate cancer. We further screened compound **12** for its effects on H3K9 dimethylation in the VCaP prostate cancer cell line. The H3K9me2 mark is a target for LSD1 in prostate cancer when in complex with the androgen receptor.[4,15] Compound **12** showed a dose-dependent increase in the H3K9me2 mark after 24 h of treatment at both 1 and 10 μM. This result suggests compound **12** shows on-target activity in cell lines as well. The fact that significant changes in histone methylation are observed at 1 μM may be the reason for the EC_{50} cluster around 1 μM in the cell viability assay for compounds with potent LSD1 biochemical activity. Further studies are needed to determine the exact mechanism of action of compound **12** in different cell lines.

Additional studies with compound **12** are currently underway to better characterize the binding mode, physicochemical attributes, and mechanism of action of these compounds including crystallographic, pharmacokinetic, and pharmacological studies. Importantly, as LSD1 activity often requires complexation with other proteins, like Co-REST, knowing the effects of inhibition on both enzymatic activity as well as complex stability is necessary to understand the pharmacology of reversible, noncompetitive inhibition with our compound series. The results presented so far lead us to conclude that

these compounds may be considered for future preclinical studies. Efforts are underway to develop additional analogues with ideal physicochemical properties for consideration in in vivo pharmacokinetic and pharmacodynamic studies.

4. CONCLUSIONS

In summary, we performed a structure-based VS of ∼2 million diverse and preprocessed compounds from a library developed in-house with the goal of identifying a novel series of LSD1 inhibitors. A novel *N*′-(1-phenylethylidene)-benzohydrazide series was identified. Optimization and exploration of the SAR were performed using both virtual and biochemical techniques. Biochemical analysis shows a specific, potent, and reversible lead compound (**12**) to take into further crystallographic, mechanistic, and pharmacological studies. These results support structure-based approaches as valid starting points for lead optimization strategies.

5. EXPERIMENTAL SECTION

5.1. Computational Methods. *5.1.1. Structure-Based Virtual Screen.* All computational studies employed PDB ID 2Z5U for the structural coordinates of LSD1.[37] Virtual screening methods from Glide, ICM, and GOLD programs were used. The protein structure was prepared by 3D protonation, deletion of water molecules, and energy minimization using the ICM force field and distance-dependent dielectric potential with an RMS gradient of 0.1; heavy atoms in the protein were kept fixed, and histidine residues were considered as neutral. VS scoring calculations utilized default parameters unless explicitly specified otherwise. PocketFinder (ICM) and SiteMap (Schroedinger) were used to define the ligand-binding site for docking studies. In both cases, the PocketFinder and SiteMap predicted ligand site is located near both the substrate and FAD-binding pockets. Default parameters in ICM include a docking site as a rectagular box with a grid spacing of 0.5 Å centered at the ligand binding site as defined by PocketFinder. A threshold set to retain 2% of the ligands along with a threshold scores of −32, maximum ligand size of 500 molecular weight, H-bond donors of 5, H-bond acceptors of 10, and torsions of 10 were used. For Glide, the default parameters similarly included the docking site as a 12 Å box centered on the geometrical center of the SiteMap-defined ligand binding site, with the ligand internal energy offset option turned on with the top 10 ranked poses for each ligand retained for scoring. Energy grids representing the active site (van der Waals, H-bonding, electrostatics, and hydrophobic interaction) were calculated with a 0.5 Å grid spacing. Confirmation of the accuracy and efficiency of the applied docking protocol used a decoy set with the adenosine phosphate fragment of FAD, the riboflavin fragment of FAD, and known LSD1 inhibitors (Chart 1) as positive controls within the Glide dl-400 1000-compound decoy set provided in the Schroedinger Suite.[42] We employed the structure-based VS to identify new small molecules which target this site on LSD1. Two separate docking runs were carried out with the ICM and Glide SP docking programs. The decoys with no valid poses after minimization were excluded from RMSD-score analysis but included in other evaluations as bad poses (GlideScore or Emodel = 10000).

The compound database was prepared using Ligprep 2.1.23 of the Schrodinger Suite and ICM's inbuilt preparation of three-dimensional (3D) ligands such that physiologically relevant protonation states were used. Prepared ligands were then docked against LSD1. Two rounds of VS, including HTVS and standard precision (SP) docking, were adopted. The top 10000 compounds ranked by Glide HTVS followed by SP were stored and submitted for additional docking experiments using Glide XP and ICM. GOLD was used only for rescoring. Specifically, the final set of 121 hits was selected based on ICM and Glide SP/XP scores as well as pharmaceutical properties predicted in QikProp, and individual compounds were visually inspected to check the docking poses and interactions between ligands and LSD1. To filter out redundant compounds, we used ICM Molcart with search criteria including compound ID, structure, and SMILES string to identify and discard the duplicates. Rescoring was performed on a minimized 121 top-ranked poses (selected from Glide SP and ICM) in Glide XP and GOLD using the "refine and do not dock" option. Finally, 121 compounds were purchased and screened in an LSD1 biochemical assay. The details of comparative docking and hit selection from ICM, Glide, and GOLD are available in the Supporting Information (Section S1).

5.1.2. Tanimoto Similarity Coefficient Calculation. Tanimoto similarity coefficients were calculated using the Molcart module of ICM.

5.2. Chemistry. All reagents and solvents were purchased from commercial sources and used without further purification. Solvents were of analytical or anhydrous grade (Sigma-Aldrich). Reactions were monitored by HPLC. Reverse phase preparative HPLC was performed using a preparative HPLC system. ^{1}H NMR spectra were recorded on a Varian Unity 400 instrument. Chemical shifts (δ) are reported in ppm downfield from solvent references. Mass spectra were obtained on a Finnegan LCQ Duo LCMS ion trap electrospray ionization (ESI) mass spectrometer. The general reaction scheme is depicted in Scheme 1, with specific reaction schemes for compounds **11**−**21** given in the Supporting Information (Figure S3). The purity of the synthesized compounds was determined by LC-MS analysis and was confirmed to be >95% purity for all biologically tested compounds.

Scheme 1. General Procedure for the Synthesis of *N*′-(1-Phenylethylidene)-benzohydrazides[a]

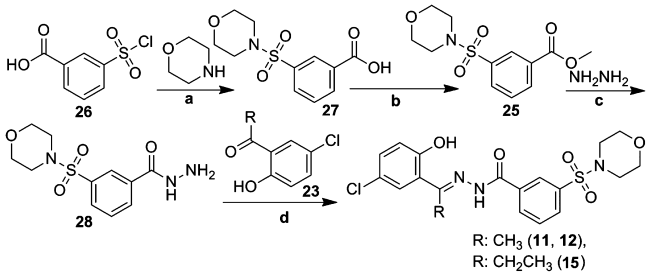

[a]Reagents and conditions: (a) THF, K_2CO_3, RT, 1 h; (b) conc H_2SO_4, CH_3OH, 65 °C, 12 h; (c) hydrazine, CH_3OH, reflux 12 h; (d) AcOH, CH_3OH, MW, 120 °C, 30 min.

5.2.1. (E)-N′-(1-(5-Chloro-2-hydroxyphenyl)ethylidene)-benzohydrazide (11). 1-(5-Chloro-2-hydroxyphenyl) ethanone **23** (100 mg, 0.586 mmol) and benzohydrazide (**24**) (80 mg, 0.586 mmol) was dissolved in methanol (4 mL) in the presence of acetic acid as a catalyst, and then the reaction mixture was heated via microwave irradiation to 120 °C for 30 min. Following cooling, the solvent was removed by vacuum and the resulting crude material was purified by Companion Rf (2% CH_3OH/CH_2Cl_2), affording the title compound **11** as a white solid (90 mg, 53%). ^{1}H NMR (400 MHz, DMSO): δ 7.95 (m, 2H), 7.67−7.62 (m, 2H), 7.56 (m, 2H), 7.35 (dd, 1H, J = 2.4 and 8.8 Hz), 6.95 (d, 1H, J = 8.4 Hz), 3.35 (s, 3H). ESI-MS: 289.0 $[M + H]^+$. LC-MS purity of compound **11** was found to be >95%.

5.2.2. (E)-N′-(1-(5-Chloro-2-hydroxyphenyl) ethylidene)-3-(morpholinosulfonyl) Benzohydrazide (12). The methyl 3-(morpholinosulfonyl) benzoate **25** was prepared in two steps. The 3-(chlorosulfonyl) benzoic acid **26** (250 mg, 1.133 mmol) was added to morpholin (99 mg, 1.133 mmol) in THF (5 mL) in presence of K_2CO_3 (313 mg, 2.266 mmol), and the resulting reaction mixture was stirred at room temperature for 1 h. After completion of the reaction from TLC, the solvents were removed and the crude material was purified by Companion Rf (3% CH_3OH/CH_2Cl_2) to give compound **27** (160 mg, 0.590 mmol) in 52% yield as white solid. In a subsequent step, compound **27** (100 mg, 0.369 mmol) dissolved in methanol (4 mL) and was added the catalytic amount of conc H_2SO_4. The resulting reaction mixture was heated to 65 °C for overnight. The solvents were removed and the crude material after purification gave **25** in 54%

dx.doi.org/10.1021/jm400870h | J. Med. Chem. 2013, 56, 9496−9508

yields (60 mg, 0.200 mmol). ^{1}H NMR (400 MHz, $CDCl_3$): δ 8.38 (t, 1H, J = 1.6 Hz), 8.27 (m, 1H), 7.92 (m, 1H), 7.64 (t, 1H, J = 8.0 Hz), 3.95 (s, 3H), 3.73 (m, 4H), 3.00 (m, 4H). ESI-MS: 286.1 $[M + H]^+$.

The methyl 3-(morpholinosulfonyl) benzoate **25** (120 mg, 0.421 mmol) was reacted with hydrazine hydrate (17.53 mg, 0.547 mmol) in methanol (5 mL) and was refluxed for 12 h at 65 °C. After completion of the reaction, solvents were removed by vacuum and the obtained crude material was purified by Companion Rf to give **28** (90 mg, 0.315 mmol, 75%). ^{1}H NMR (400 MHz, $CDCl_3$): δ 8.16 (m, 1H), 8.12 (m, 1H), 8.04 (m, 1H), 7.85 (m, 1H), 7.63 (t, 1H, J = 8.0 Hz), 4.19 (m, 2H), 3.71 (m, 4H), 2.97 (m,4H). ESI-MS: 286.1 $[M + H]^+$.

In the final step, either the ester compound **25** or 3-(morpholinosulfonyl) benzoic acid **27** was utilized for the preparation of series of benzohydrazide compounds. In one example starting with 1-(5-chloro-2-hydroxyphenyl) ethanone **23** (25.2 mg, 0.147 mmol) and hydrazine **28** (4.72 mg, 0.147 mmol) was refluxed in methanol (5 mL) in the presence of catalytic acetic acid for 1 h. In certain examples, the microwave heating to 120 °C for 30 min was performed. After completion of the reaction, the solvents was removed by vacuum and the resulting crude material was purified by Companion Rf with 2% CH_3OH/CH_2Cl_2 affording the title, in this case the compound **12** as a white solid (85%). ^{1}H NMR (400 MHz, DMSO-d_6): δ 13.31 (s, 1H), 11.69 (s, 1H), 8.27 (d, 1H, J = 7.6 Hz), 8.18 (s, 1H), 7.96 (d, 1H, J = 7.6 Hz), 7.83 (t, 1H, J = 7.6 Hz), 7.65 (d, 1H, J = 2.4 Hz), 7.33 (dd, 1H, J = 2.4 and 8.4 Hz), 6.94 (d, 1H, J = 9.2 Hz), 3.62 (m, 4H), 2.90 (m, 4H), 2.49 (s, 3H). ^{13}C NMR (100 MHz, DMSO-d_6): δ 164.0, 158.4, 158.1, 135.5, 134.8, 133.7, 131.7, 131.5, 1.30.5, 128.6, 127.8, 122.8, 121.4, 119.8, 65.9, 46.6, 15.1. HRMS: expected 438.0885 [M + H], observed 438.0898 [M + H]. LC-MS purity of compound **12** was found to be >95%.

Similar experimental procedures were employed for the preparation of list of compounds given in Table 2, and their NMR and mass spectral data confirms the title compounds.

*5.2.3. (E)-N′-(1-(2,5-Dichlorophenyl)ethylidene)-3-(morpholinosulfonyl)benzohydrazide (**13**).* 1-(2,5-Dichlorophenyl)-ethanone **29** (20 mg, 0.106 mmol) and 3-(morpholinosulfonyl) benzohydrazide **28** (30.2 mg, 0.106 mmol) was dissolved in methanol (volume: 4 mL) in the presence of acetic acid as a catalyst, and then the reaction mixture was heated via microwave irradiation to 120 °C for 30 min. Following cooling, the solvent was removed by vacuum and the resulting crude material was purified by Companion Rf with 1% CH_3OH/CH_2Cl_2, affording the title compound **13** as a solid (10 mg, 21%). ^{1}H NMR (400 MHz, $CDCl_3$): δ 8.29 (m, 1H), 8.09 (m, 1H), 7.81 (m, 1H), 7.57 (m, 1H), 7.40 (m, 1H), 7.26 (m, 2H), 3.52 (m, 4H), 2.91 (m, 4H), 2.28 (s, 3H). ESI-MS: 456.1 $[M + H]^+$. LC-MS purity of compound **13** was found to be >95%.

*5.2.4. (Z)-3-(2-(1-(5-Chloro-2-hydroxyphenyl)ethylidene)-hydrazinecarbonyl)-N,N-dimethylbenzenesulfonamide (**14**).* 3-(*N*,*N*-Dimethylsulfamoyl)benzoic acid (200 mg, 0.872 mmol) was refluxed in the presence of conc H_2SO_4 (5.64 mg, 0.044 mmol) in methanol at 70 °C for overnight, and after completion of the reaction, solvent was removed by vacuum and then compound was purified by Companion Rf with 1% CH_3OH/CH_2Cl_2, affording the methyl 3-(*N*,*N*-dimethylsulfamoyl)benzoate **30** as a solid (125 mg, 58.9%). ^{1}H NMR (400 MHz, $CDCl_3$): δ 8.42 (s, 1H), 8.27 (d, 1H, J = 8.0 Hz), 7.97 (d, 1H, J = 7.2 Hz), 7.65 (t, 1H, J = 8.0 Hz), 3.96 (s, 3H), 2.74 (s, 6H). ESI-MS: 244.0 $[M + H]^+$.

Methyl 3-(*N*,*N*-dimethylsulfamoyl)-benzoate **30** (150 mg, 0.617 mmol) was added to the hydrazine (29.6 mg, 0.925 mmol) in methanol and refluxed for 8 h at 65 °C. Following cooling, reaction was monitored by TLC. After completion of the reaction, solvent was removed by vacuum and then compound was purified by Companion Rf with 1% CH_3OH/CH_2Cl_2, affording the 3-(hydrazinecarbonyl)-*N*,*N*-dimethylbenzenesulfonamide **31** as a solid (60 mg, 40%). ^{1}H NMR (400 MHz, $CDCl_3$): δ 8.11 (s, 1H), 8.01 (d, 1H, J = 8.4 Hz), 7.92 (d, 1H, J = 8.0 Hz), 7.65 (t, 1H, J = 8.0 Hz), 2.73 (s, 6H). ESI-MS: 244.0 $[M + H]^+$.

3-(Hydrazinecarbonyl)-*N*,*N*-dimethylbenzenesulfonamide **31** (50 mg, 0.206 mmol) and 1-(5-chloro-2-hydroxyphenyl)ethanone **23** (35.1 mg, 0.206 mmol) was dissolved in methanol (volume: 4 mL) in the presence of acetic acid as a catalyst, and then the reaction mixture was heated via microwave irradiation to 120 °C for 30 min. Reaction was monitored by TLC. After completion of the reaction, following cooling, the solvent was removed by vacuum and the resulting crude material was purified by Companion Rf with 1% CH_3OH/CH_2Cl_2, afforded the title compound **14** as a solid (15 mg, 18%). ^{1}H NMR (400 MHz, acetone-d_6): δ 8.29 (m, 2H), 8.01 (d, 1H, J = 8.4 Hz), 7.83 (t, 1H, J = 8.4 Hz), 7.62 (d, 1H, J = 2.4 Hz), 7.32 (dd, 1H, J = 2.4 and 8.8 Hz), 6.96 (d, 1H, J = 8.8 Hz), 2.73 (s, 6H), 2.58 (s, 3H). ESI-MS: 396.0 $[M + H]^+$. LC-MS purity of compound **14** was found to be >95%.

*5.2.5. (Z)-N′-(1-(5-Chloro-2-hydroxyphenyl)propylidene)-3-(morpholinosulfonyl)benzohydrazide (**15**).* 3-(Morpholinosulfonyl)-benzohydrazide **28** (40 mg, 0.140 mmol) and 1-(5-chloro-2-hydroxyphenyl)propan-1-one **32** (25.9 mg, 0.140 mmol) was dissolved in methanol (volume: 4 mL) in the presence of acetic acid as a catalyst, and then the reaction mixture was heated via microwave irradiation to 120 °C for 30 min. Reaction was monitored by TLC. After completion of the reaction, following cooling, the solvent was removed by vacuum and the resulting crude material was purified by Companion Rf with 2% CH_3OH/CH_2Cl_2, affording the title compound **15** as a solid (20 mg, 31.6%). ^{1}H NMR (400 MHz, acetone-d_6): δ 8.26 (m, 2H), 8.00 (d, 1H, J = 7.6 Hz), 7.84 (t, 1H, J = 8.0 Hz), 7.64 (d, 1H, J = 2.4 Hz), 7.33 (m, 1H), 6.98 (d, 1H, J = 9.2 Hz), 3.69 (m, 4H), 3.10 (q, 2H, J = 7.6 Hz), 2.99 (m, 4H), 1.26 (t, 3H, J = 7.6 Hz). ESI-MS: 452.1 $[M + H]^+$. LC-MS purity of compound **15** was found to be >95%.

*5.2.6. (E)-N′-(1-(3-Chloro-2-fluorophenyl)ethylidene)-3-(morpholinosulfonyl)benzohydrazide (**16**).* 1-(3-Chloro-2-fluorophenyl)ethanone **33** (20 mg, 0.116 mmol) and 3-(morpholino-sulfonyl) benzohydrazide **28** (33.1 mg, 0.116 mmol) was dissolved in methanol (4 mL) in the presence of acetic acid as a catalyst, and then the reaction mixture was heated via microwave irradiation to 120 °C for 30 min. Following cooling, the solvent was removed by vacuum, and the resulting crude material was purified by Companion Rf with 2% CH_3OH/CH_2Cl_2, affording the title compound **16** as a white solid (22 mg, 43.2%). ^{1}H NMR (400 MHz, $CDCl_3$): δ 9.34 (s, 1H), 8.37 (m, 1H), 8.16 (m, 1H), 7.87 (d, 1H, J = 7.2 Hz), 7.65 (m, 1H), 7.41 (m, 1H), 7.10 (t, 1H, J = 8.0 Hz), 3.71 (m, 4H), 2.95 (m, 4H), 2.38 (s, 3H). ESI-MS: 440.1 $[M + H]^+$. LC-MS purity of compound **16** was found to be >95%.

*5.2.7. (E)-N′-(1-(2,6-Dihydroxyphenyl)ethylidene)benzohydrazide (**17**).* 1-(2,6-Dihydroxyphenyl)ethanone (100 mg, 0.657 mmol) **34** and benzohydrazide **24** (89 mg, 0.657 mmol) was dissolved in methanol (4 mL) in the presence of acetic acid as a catalyst, and then the reaction mixture was heated via microwave irradiation to 120 °C for 30 min. Following cooling, the solvent was removed by vacuum and the resulting crude material was purified by Companion Rf with 2% CH_3OH/CH_2Cl_2, affording the title compound **17** as a white solid (100 mg, 56.3%). ^{1}H NMR (400 MHz, CD_3OD): δ 7.59 (m, 2H), 7.49 (m, 1H), 7.39 (m, 2H), 7.11 (t, 1H, J = 8.0 Hz), 6.45 (m, 2H), 2.35 (s, 3H). ESI-MS: 271.1 $[M + H]^+$. LC-MS purity of compound **17** was found to be >95%.

*5.2.8. (E)-N′-(1-(2-Chloropyridin-4-yl)ethylidene)-3-(morpholinosulfonyl)benzohydrazide (**18**).* 1-(2-Chloropyridin-4-yl)-ethanone **35** (20 mg, 0.129 mmol) and 3-(morpholinosulfonyl)-benzohydrazide **28** (36.7 mg, 0.129 mmol) was dissolved in methanol (4 mL) in the presence of acetic acid as a catalyst, and then the reaction mixture was heated via microwave irradiation to 120 °C for 30 min. Following cooling, the solvent was removed by vacuum and the resulting crude material was purified by Companion Rf with 1% CH_3OH/CH_2Cl_2, affording the title compound **18** as a solid (32.6 mg, 60%). ^{1}H NMR (400 MHz, $CDCl_3$): δ 9.43 (m, 1H), 8.39 (m, 2H), 8.15 (d, 1H, J = 8.0 Hz), 7.93 (d, 1H, J = 7.6 Hz), 7.70 (t, 1H, J= 7.6 Hz), 7.52 (m, 1H), 3.73 (m, 4H), 3.02 (m, 4H), 2.35 (s, 3H). ESI-MS: 423.1 $[M + H]^+$. LC-MS purity of compound 18 was found to be >95%.

*5.2.9. (Z)-3-Bromo-4-chloro-N′-(1-(5-chloro-2-hydroxyphenyl)-ethylidene)benzohydrazide (**19**).* 3-Bromo-4-chlorobenzoic acid (200 mg, 0.849 mmol) was refluxed in the presence of conc H_2SO_4 (5.49 mg, 0.042 mmol) in methanol at 70 °C for overnight, and after

dx.doi.org/10.1021/jm400870h | J. Med. Chem. 2013, 56, 9496−9508

completion of the reaction, solvent was removed by vacuum and then compound was purified by Companion Rf with 1% CH_3OH/CH_2Cl_2, affording the methyl 3-bromo-4-chlorobenzoate **36** as a white solid (130 mg, 61.3%). ^{1}H NMR (400 MHz, $CDCl_3$): δ 8.29 (d, 1H, J = 2.0 Hz), 7.91 (dd, 1H, J = 2.0 and 8.4 Hz), 7.52 (d, 1H, J = 8.4 Hz), 3.92 (s, 3H). ESI-MS: 250.9 $[M + H]^+$.

Compound **36** (120 mg, 0.481 mmol) was added to the hydrazine (23.12 mg, 0.721 mmol) in methanol at 70 °C for overnight. Reaction was monitored by TLC. After completion of the reaction, solvent was removed by vacuum and then compound was purified by Companion Rf with 2% CH_3OH/CH_2Cl_2, affording the intermediate 3-bromo-4-chlorobenzohydrazide **37** as a solid (30 mg, 25%). ^{1}H NMR (400 MHz, $CDCl_3$): δ 8.02 (d, 1H, J = 1.6 Hz), 7.60 (dd, 1H, J = 2.0 and 8.0 Hz), 7.52 (d, 1H, J = 8.0 Hz). ESI-MS: 250.9 $[M + H]^+$.

The compound **37** (30 mg, 0.120 mmol) and 1-(5-chloro-2-hydroxyphenyl)ethanone **23** (20.51 mg, 0.120 mmol) was dissolved in methanol (volume: 4 mL) in the presence of acetic acid as a catalyst, and then the reaction mixture was heated via microwave irradiation to 120 °C for 30 min. Reaction was monitored by TLC. After completion of the reaction, following cooling, the solvent was removed by vacuum and the resulting crude material was purified by Companion Rf with 2% CH_3OH/CH_2Cl_2, affording the title compound **19** as a solid (15 mg, 31%). ^{1}H NMR (400 MHz, acetone-d_6): δ 8.30 (s, 1H), 7.98 (d, 1H, J = 8.4 Hz), 7.73 (d, 1H, J = 8.4 Hz), 7.61 (d, 1H, J = 2.4 Hz), 7.29 (dd, 1H, J = 2.4 and 8.4 Hz), 6.93 (d, 1H, J = 8.8 Hz), 2.55 (s, 3H). ESI-MS: 402.9 $[M + H]^+$. LC-MS purity of compound **19** was found to be >95%.

*5.2.10. (Z)-5-Bromo-6-chloro-N′-(1-(5-chloro-2-hydroxyphenyl)-ethylidene)nicotinohydrazide (**20**).* Methyl 5-bromo-6-chloronicotinate (100 mg, 0.399 mmol) was added to the hydrazine (19.19 mg, 0.599 mmol) in methanol at 70 °C for overnight. Reaction was monitored by TLC. After completion of the reaction, solvent was removed by vacuum and then compound was purified by Companion Rf with 1% CH_3OH/CH_2Cl_2, affording the 5-bromo-6-chloronicotinohydrazide **38** as a solid (20 mg, 20%). ^{1}H NMR (400 MHz, CD_3OD): δ 8.33 (d, 1H, J = 2.4 Hz), 8.01 (d, 1H, J = 2.4 Hz).

5-Bromo-6-chloronicotinohydrazide **38** (15 mg, 0.060 mmol) and 1-(5-chloro-2-hydroxyphenyl)ethanone **23** (10.22 mg, 0.060 mmol) was dissolved in methanol (volume: 4 mL) in the presence of acetic acid as a catalyst, and then the reaction mixture was heated via microwave irradiation to 120 °C for 30 min. Reaction was monitored by TLC. After completion of the reaction, following cooling, the solvent was removed by vacuum and the resulting crude material was purified by Companion Rf with 2% CH_3OH/CH_2Cl_2, affording the title compound **20** as a solid (8 mg, 33%). ^{1}H NMR (400 MHz, DMSO-d_6): δ 8.39 (d, 1H, J = 2.4 Hz), 8.28 (s, 1H), 7.63 (d, 1H, J = 2.4 Hz), 7.32 (dd, 1H, J = 2.4 and 8.8 Hz), 7.06 (d, 1H, J = 6.8 Hz), 6.92 (d, 1H, J = 9.2 Hz), 6.81 (d, 1H, J = 6.8 Hz), 2.47 (s, 3H). ESI-MS: 404.0 $[M + H]^+$. LC-MS purity of compound 20 was found to be >95%.

*5.2.11. (Z)-5-Chloro-N′-(1-(5-chloro-2-hydroxyphenyl)-ethylidene)nicotinohydrazide (**21**).* 5-Chloronicotinic acid (200 mg, 1.269 mmol) was refluxed in the presence of conv H_2SO_4 (8.20 mg, 0.063 mmol) in methanol at 70 °C for overnight, and after completion of the reaction, solvent was removed by vacuum and then compound was purified by Companion Rf with 1% CH_3OH/CH_2Cl_2, affording the methyl 5-chloronicotinate **39** as a solid (120 mg, 55%). ^{1}H NMR (400 MHz, $CDCl_3$): δ 9.07 (d, 1H, J = 1.6 Hz), 8.72 (d, 1H, J = 2.0 Hz), 8.26 (m, 1H), 3.95 (s, 1H).

Hydrazine (17.93 mg, 0.560 mmol) was added to the methyl 5-chloronicotinate **39** (80 mg, 0.466 mmol) in methanol at 70 °C overnight. Reaction was monitored by TLC. After completion of the reaction, solvent was removed by vacuum and then compound was purified by Companion Rf with 1% CH_3OH/CH_2Cl_2, affording the 5-chloronicotinohydrazide **40** as a solid (40 mg, 50%). ^{1}H NMR (400 MHz, CD_3OD): δ 8.85 (d, 1H, J = 2.0 Hz), 8.70 (d, 1H, J = 2.4 Hz), 8.22 (t, 1H, J = 2.0 Hz). ESI-MS: 172.0 $[M + H]^+$.

5-chloronicotinohydrazide **40** (30 mg, 0.175 mmol) and 1-(5-chloro-2-hydroxyphenyl)ethanone **23** (29.8 mg, 0.175 mmol) was dissolved in methanol (volume: 4 mL) in the presence of acetic acid as a catalyst, and then the reaction mixture was heated via microwave irradiation to 120 °C for 30 min. Reaction was monitored by TLC. After completion of the reaction, following cooling, the solvent was removed by vacuum and the resulting crude material was purified by Companion Rf with 2% CH_3OH/CH_2Cl_2, affording the title compound **21** as a solid (20 mg, 35.3%). ^{1}H NMR (400 MHz, acetone-d_6): δ 9.06 (s, 1H), 8.77 (s, 1H), 8.37 (s, 1H), 7.62 (d, 1H, J = 2.8 Hz), 7.31 (dd, 1H, J = 2.0 and 8.4 Hz), 6.95 (d, 1H, J = 8.8 Hz), 2.58 (s, 3H). ESI-MS: 324.0 $[M + H]^+$. LC-MS purity of compound **21** was found to be >95%.

*5.2.12. (Z)-3-(Morpholinosulfonyl)-N′-(1-(pyridin-3-yl)-ethylidene)benzohydrazide (**22**).* 3-(Morpholino sulfonyl)-benzohydrazide **28** (40 mg, 0.140 mmol) and 1-(pyridin-3-yl)-ethanone **41** (16.98 mg, 0.140 mmol) was dissolved in methanol (4 mL) in the presence of acetic acid as a catalyst, and then the reaction mixture was heated via microwave irradiation to 120 °C for 30 min. Reaction was monitored by TLC. After completion of the reaction, following cooling, the solvent was removed by vacuum and the resulting crude material was purified by Companion Rf with 2% CH_3OH/CH_2Cl_2, affording the title compound **22** as a solid (15 mg, 27.5%). ^{1}H NMR (400 MHz, $CDCl_3$): δ 9.53 (bs, 1H), 8.87 (s, 1H), 8.59 (m, 1H), 8.39 (m, 1H), 8.17 (m, 1H), 7.98 (m, 1H), 7.89 (d, 1H, J = 8.0 Hz), 7.67 (t, 1H, J = 8.0 Hz), 7.32 (m, 1H), 3.70 (m, 4H), 3.00 (m, 4H), 2.39 (s, 3H). ESI-MS: 389.0 $[M + H]^+$. LC-MS purity of compound **22** was found to be >95%.

5.3. Biochemical Assays. *5.3.1. LSD1 Screening Assay.* The LSD1 screening biochemical assay kit was purchased from Cayman Chemical (Ann Arbor, MI). Test compounds were diluted to 20× the desired test concentration in 100% DMSO and 2.5 μL of the diluted drug sample was added to a black 384-well plate. The LSD1 enzyme stock was diluted 17-fold with assay buffer, and 40 μL of the diluted LSD1 enzyme was added to the appropriate wells. Substrate, consisting of horseradish peroxidase, dimethyl K4 peptide corresponding to the first 21 amino acids of the N-terminal tail of histone H3, and 10-acetyl-3,7-dihydroxyphenoxazine was then added to wells. Resorufin was analyzed on an Envision plate reader with an excitation wavelength of 530 nm and an emission wavelength of 595 nm.

5.3.2. Off-Target Assays. Monoamine oxidase A and B enzymes were purchased from Sigma (catalogue nos. m7316, and m7441, respectively). Biochemical kits were purchased as follows: MAO-Glo − Promega Corp. (Fitchburg, WI); D-lactate dehydrogenase, Cayman Chemical (Ann Arbor, MI); glucose oxidase, Life Technologies Corp. (Grand Island, NY). Inhibition assay were carried out according to the manufacturer's suggested protocol. CYP and hERG evaluation utilized the SelectScreen Biochemical P450 Profiling and hERG Screening Services provided by Invitrogen Corp. (Madison, WI).

5.3.3. Reversibility and Michaelis−Menten Analysis. Biochemical characterization of reversibility and K_i was performed using the biochemical screen from Cayman Chemical with purified recombinant full-length his_6-LSD1 substituted for the commercially provided protein mix. Reversibility was determined using jump dilution. LSD1 was incubated at 10× IC_{50} of compound **12** or tranylcypromine for 1 h then diluted into the reaction 100-fold. The reaction buffer was either compound-free or contained 10× the IC_{50}. Compound **13** was used as a negative control. The K_i of compound **12** was determined using a Michaelis−Menten kinetic analysis across multiple concentrations of compound **12**. The data was plotted in GraphPad. K_i was determined using the following equation: $K_i = [\text{Inhibitor}]/((v_{max}/v_{\text{apparent-max}}) - 1)$

5.4. In Vitro Assays. *5.4.1. ATPlite Cell Viability A.* ATPlite was purchased from PerkinElmer (Waltham, MA). Cancer cell lines were obtained from ATCC. Cells were cultured according to the procedures provided. Cells were seeded in 96-well plates and then treated with different concentrations of inhibitor (0.1% final DMSO concentration). After 96 h of incubation, ATPlite was added directly to the culture well. Luminescence was read 5 min later on an Envision plate reader.

5.4.2. Global H3K4 and H3K9 Methylation Analysis. VCaP cells were maintained in RPMI media containing 10% FBS and no phenol red. The day before the experiment was started, we plated 500000 cells per well of a 12-well plate. The following day, the culture medium was

dx.doi.org/10.1021/jm400870h | J. Med. Chem. 2013, 56, 9496−9508

replaced with fresh RPMI containing 10% FBS and compound **12**. Individual compound **12** solutions were prepared using DMSO; the final concentration of the solvent in the culture medium was 1%. The cells then were incubated for 24 h at 37 °C. Individual wells were washed with PBS, and lysates were obtained as described previously.[43] We subjected 50 μg of total protein to electrophoresis and immunoblot analyses using anti-H3K9Me2 and anti-β-Actin antibodies, as described.[37] The extent of immunoreactivity then was assessed by chemiluminescence, following incubation with appropriate, horseradish peroxidase-labeled, secondary antibodies.

■ ASSOCIATED CONTENT

Supporting Information

Detailed virtual screening methods; purchased hits, analytical data; docking scores of compounds **1**−**10**, commercially available LSD1 hits (111) from the list of 121 compounds selected, Tanimoto similarity coefficients comparing compound **12** and known LSD1 inhibitors from Chart 1; off-target inhibition; comparison of different model fits for enzyme kinetics; binding site model and definition of active site of LSD1 structure; flow diagram for the virtual ligand screening (VLS) using ICM-VLS; Schrodinger workflow GOLD programs; complete reaction schemes for compounds **11**−**22**; LC-MS data for compound **12**. This material is available free of charge via the Internet at http://pubs.acs.org.

■ AUTHOR INFORMATION

Corresponding Author

*Phone: +1-(801)587-5559. Fax: +1-(801)585-0101. E-mail: sunil.sharma@hci.utah.edu. Address: Huntsman Cancer Institute, Room 3360, 2000 Circle of Hope, Salt Lake City, Utah 84112, United States.

Author Contributions

⊥These authors contributed equally.

Notes

The authors declare the following competing financial interest(s): Drs. Sunil Sharma, David Bearss, Steve Warner, and Hariprasad Vankayalapati have equity interest in Salarius Pharmaceuticals.

■ ACKNOWLEDGMENTS

We gratefully acknowledge Dr. Yang Shi for the generous gift of the LSD1 expression construct, Dr. Diana Stafforini for her assistance with VCaP cell culture and blots, and Jedediah Doane, Simon Currie, Dr. Niraja Bhachech, and Dr. Barbara Graves for their protein purification guidance. Research reported in this article utilized the Experimental Therapeutics program and was supported by the Huntsman Cancer Foundation and the National Cancer Institute of the National Institutes of Health under award number P30CA042014. The content is solely the responsibility of the authors and does not necessarily represent the official views of the NIH.

■ ABBREVIATIONS USED

BHC80, BRAF35-HDAC complex protein 80; Co-REST, REST corepressor 1; CYP, cytochrome P450; DSF, differential scanning fluorimetry; FAD, flavin adenine dinucleotide; Gfi-1, growth factor independent 1; H3, histone H3; H3K4, histone H3 at lysine 4; H3K4me1, monomethylation of histone H3 at lysine 4; H3K4me2, dimethylation of histone H3 at lysine 4; H3K4me3, trimethylation of histone H3 at lysine 4; H3K9, histone H3 at lysine 9; H3K9me1, monomethylation of histone H3 at lysine 9; H3K9me2, dimethylation of histone H3 at lysine 9; HDAC, histone deacetylase; hERG, human ether-à-go-go; HTVS, high-throughput virtual screen; K4, lysine 4; K9, lysine 9; LSD1, lysine-specific demethylase; MAO, monoamine oxidase; NuRD, nucleosome remodeling and histone deacetylase; SAR, structure−activity relationship; SNAI1, snail homologue 1 (drosophila); TCP, tranylcypromine; VS, virtual screen

■ REFERENCES

(1) Tsai, H.-C.; Baylin, S. B. Cancer epigenetics: linking basic biology to clinical medicine. *Cell Res.* **2011**, *21*, 502−517.

(2) Füllgrabe, J.; Kavanagh, E.; Joseph, B. Histone onco-modifications. *Oncogene* **2011**, *30*, 3391−3403.

(3) Shi, Y.; Lan, F.; Matson, C.; Mulligan, P.; Whetstine, J. R.; Cole, P. A.; Casero, R. A.; Shi, Y. Histone Demethylation Mediated by the Nuclear Amine Oxidase Homolog LSD1. *Cell* **2004**, *119*, 941−953.

(4) Metzger, E.; Wissmann, M.; Yin, N.; Müller, J. M.; Schneider, R.; Peters, A. H. F. M.; Günther, T.; Buettner, R.; Schüle, R. LSD1 demethylates repressive histone marks to promote androgen-receptor-dependent transcription. *Nature* **2005**, *437*, 436−439.

(5) Jenuwein, T.; Allis, C. D. Translating the Histone Code. *Science* **2001**, *293*, 1074−1080.

(6) Lachner, M.; O'Sullivan, R. J.; Jenuwein, T. An epigenetic road map for histone lysine methylation. *J. Cell Sci.* **2003**, *116*, 2117−2124.

(7) Forneris, F.; Binda, C.; Vanoni, M. A.; Mattevi, A.; Battaglioli, E. Histone demethylation catalysed by LSD1 is a flavin-dependent oxidative process. *FEBS Lett.* **2005**, *579*, 2203−2207.

(8) Forneris, F.; Binda, C.; Battaglioli, E.; Mattevi, A. LSD1: oxidative chemistry for multifaceted functions in chromatin regulation. *Trends Biochem. Sci.* **2008**, *33*, 181−189.

(9) Yang, M.; Gocke, C. B.; Luo, X.; Borek, D.; Tomchick, D. R.; Machius, M.; Otwinowski, Z.; Yu, H. Structural Basis for CoREST-Dependent Demethylation of Nucleosomes by the Human LSD1 Histone Demethylase. *Mol. Cell* **2006**, *23*, 377−387.

(10) Shi, Y.-J.; Matson, C.; Lan, F.; Iwase, S.; Baba, T.; Shi, Y. Regulation of LSD1 Histone Demethylase Activity by Its Associated Factors. *Mol. Cell* **2005**, *19*, 857−864.

(11) Lan, F.; Collins, R. E.; De Cegli, R.; Alpatov, R.; Horton, J. R.; Shi, X.; Gozani, O.; Cheng, X.; Shi, Y. Recognition of unmethylated histone H3 lysine 4 links BHC80 to LSD1-mediated gene repression. *Nature* **2007**, *448*, 718−722.

(12) Lee, M. G.; Wynder, C.; Cooch, N.; Shiekhattar, R. An essential role for CoREST in nucleosomal histone 3 lysine 4 demethylation. *Nature* **2005**, *437*, 432−435.

(13) Forneris, F.; Binda, C.; Dall'Aglio, A.; Fraaije, M. W.; Battaglioli, E.; Mattevi, A. A Highly Specific Mechanism of Histone H3-K4 Recognition by Histone Demethylase LSD1. *J. Biol. Chem.* **2006**, *281*, 35289−35295.

(14) Forneris, F.; Binda, C.; Vanoni, M. A.; Battaglioli, E.; Mattevi, A. Human Histone Demethylase LSD1 Reads the Histone Code. *J. Biol. Chem.* **2005**, *280*, 41360−41365.

(15) Garcia-Bassets, I.; Kwon, Y.-S.; Telese, F.; Prefontaine, G. G.; Hutt, K. R.; Cheng, C. S.; Ju, B.-G.; Ohgi, K. A.; Wang, J.; Escoubet-Lozach, L.; Rose, D. W.; Glass, C. K.; Fu, X.-D.; Rosenfeld, M. G. Histone Methylation-Dependent Mechanisms Impose Ligand Dependency for Gene Activation by Nuclear Receptors. *Cell* **2007**, *128*, 505−518.

(16) Lim, S.; Janzer, A.; Becker, A.; Zimmer, A.; Schüle, R.; Buettner, R.; Kirfel, J. Lysine-specific demethylase 1 (LSD1) is highly expressed in ER-negative breast cancers and a biomarker predicting aggressive biology. *Carcinogenesis* **2010**, *31*, 512−520.

(17) Schulte, J. H.; Lim, S.; Schramm, A.; Friedrichs, N.; Koster, J.; Versteeg, R.; Ora, I.; Pajtler, K.; Klein-Hitpass, L.; Kuhfittig-Kulle, S.; Metzger, E.; Schüle, R.; Eggert, A.; Buettner, R.; Kirfel, J. Lysine-Specific Demethylase 1 Is Strongly Expressed in Poorly Differentiated Neuroblastoma: Implications for Therapy. *Cancer Res.* **2009**, *69*, 2065−2071.

(18) Hayami, S.; Kelly, J. D.; Cho, H.-S.; Yoshimatsu, M.; Unoki, M.; Tsunoda, T.; Field, H. I.; Neal, D. E.; Yamaue, H.; Ponder, B. A. J.; Nakamura, Y.; Hamamoto, R. Overexpression of LSD1 contributes to human carcinogenesis through chromatin regulation in various cancers. *Int. J. Cancer* **2011**, *128*, 574−586.
(19) Kahl, P.; Gullotti, L.; Heukamp, L. C.; Wolf, S.; Friedrichs, N.; Vorreuther, R.; Solleder, G.; Bastian, P. J.; Ellinger, J.; Metzger, E.; Schüle, R.; Buettner, R. Androgen Receptor Coactivators Lysine-Specific Histone Demethylase 1 and Four and a Half LIM Domain Protein 2 Predict Risk of Prostate Cancer Recurrence. *Cancer Res.* **2006**, *66*, 11341−11347.
(20) Zhao, Z.-K.; Yu, H.-F.; Wang, D.-R.; Dong, P.; Chen, L.; Wu, W.-G.; Ding, W.-J.; Liu, Y.-B. Overexpression of lysine specific demethylase 1 predicts worse prognosis in primary hepatocellular carcinoma patients. *World J. Gastroenterol.* **2012**, *18*, 6651−6656.
(21) Huang, Y.; Stewart, T. M.; Wu, Y.; Baylin, S. B.; Marton, L. J.; Perkins, B.; Jones, R. J.; Woster, P. M.; Casero, R. A. Novel oligoamine analogues inhibit lysine-specific demethylase 1 (LSD1) and induce re-expression of epigenetically silenced genes. *Clin. Cancer Res.* **2009**, *15*, 7217−7228.
(22) Liang, Y.; Quenelle, D.; Vogel, J. L.; Mascaro, C.; Ortega, A.; Kristie, T. M. A Novel Selective LSD1/KDM1A Inhibitor Epigenetically Blocks Herpes Simplex Virus Lytic Replication and Reactivation from Latency. *mBio* **2013**, *4*, 00558-12.
(23) Mimasu, S.; Umezawa, N.; Sato, S.; Higuchi, T.; Umehara, T.; Yokoyama, S. Structurally Designed *trans*-2-Phenylcyclopropylamine Derivatives Potently Inhibit Histone Demethylase LSD1/KDM1. *Biochemistry* **2010**, *49*, 6494−6503.
(24) Binda, C.; Valente, S.; Romanenghi, M.; Pilotto, S.; Cirilli, R.; Karytinos, A.; Ciossani, G.; Botrugno, O. A.; Forneris, F.; Tardugno, M.; Edmondson, D. E.; Minucci, S.; Mattevi, A.; Mai, A. Biochemical, Structural, and Biological Evaluation of Tranylcypromine Derivatives as Inhibitors of Histone Demethylases LSD1 and LSD2. *J. Am. Chem. Soc.* **2010**, *132*, 6827−6833.
(25) Ueda, R.; Suzuki, T.; Mino, K.; Tsumoto, H.; Nakagawa, H.; Hasegawa, M.; Sasaki, R.; Mizukami, T.; Miyata, N. Identification of Cell-Active Lysine Specific Demethylase 1-Selective Inhibitors. *J. Am. Chem. Soc.* **2009**, *131*, 17536−17537.
(26) Ortega, A. M.; Castro-Palomino, L. J.; Fyfe, M. C. T. Lysine specific demethylase inhibitors and their use. PCT Int. Appl. WO 2011035941 A12011.
(27) Guibourt, N.; Ortega, A. M.; Castro-Palomino, L. J. Phenylcyclopropylamine derivatives and their medical use. PCT Int. Appl. , WO 2010084160 A1, 2010.
(28) Guibourt, N.; Ortega, A. M.; Castro-Palomino, L. J. Oxidase inhibitors and their use. PCT Int. Appl. WO 2010043721 A1, 2010.
(29) McCafferty, D. G.; Pollock, J. Arylcyclopropylamines and methods of use. PCT Int. Appl. US 20100324147 A1, 2010.
(30) Culhane, J. C.; Szewczuk, L. M.; Liu, X.; Da, G.; Marmorstein, R.; Cole, P. A. A Mechanism-Based Inactivator for Histone Demethylase LSD1. *J. Am. Chem. Soc.* **2006**, *128*, 4536−4537.
(31) Culhane, J. C.; Wang, D.; Yen, P. M.; Cole, P. A. Comparative Analysis of Small Molecules and Histone Substrate Analogs as LSD1 Lysine Demethylase Inhibitors. *J. Am. Chem. Soc.* **2010**, *132*, 3164−3176.
(32) Sharma, S. K.; Wu, Y.; Steinbergs, N.; Crowley, M. L.; Hanson, A. S.; Casero, R. A.; Woster, P. M. (Bis)urea and (Bis)thiourea Inhibitors of Lysine-Specific Demethylase 1 as Epigenetic Modulators. *J. Med. Chem.* **2010**, *53*, 5197−5212.
(33) Huang, Y.; Greene, E.; Murray Stewart, T.; Goodwin, A. C.; Baylin, S. B.; Woster, P. M.; Casero, R. A. Inhibition of lysine-specific demethylase 1 by polyamine analogues results in reexpression of aberrantly silenced genes. *Proc. Natl. Acad. Sci. U. S. A.* **2007**, *104*, 8023−8028.
(34) Wang, J.; Lu, F.; Ren, Q.; Sun, H.; Xu, Z.; Lan, R.; Liu, Y.; Ward, D.; Quan, J.; Ye, T.; Zhang, Hui. Novel Histone Demethylase LSD1 Inhibitors Selectively Target Cancer Cells with Pluripotent Stem Cell Properties. *Cancer Res.* **2011**, *71*, 7238−7249.
(35) Willmann, D.; Lim, S.; Wetzel, S.; Metzger, E.; Jandausch, A.; Wilk, W.; Jung, M.; Forne, I.; Imhof, A.; Janzer, A.; Kirfel, J.; Waldmann, H.; Schüle, R.; Buettner, R. Impairment of prostate cancer cell growth by a selective and reversible lysine-specific demethylase 1 inhibitor. *Int. J. Cancer* **2012**, *131*, 2704−2709.
(36) Vankayalapati, H.; Sorna, V.; Warner, S. L.; Bearss, D. J.; Sharma, S.; Stephens, B. Substituted (*E*)-*N*′-(1-phenylethylidene) benzohydrazide analogs as histone demethylase inhibitors. PCT Int. Appl. WO 2013025805 A1, 2013.
(37) Mimasu, S.; Sengoku, T.; Fukuzawa, S.; Umehara, T.; Yokoyama, S. Crystal structure of histone demethylase LSD1 and tranylcypromine at 2.25 Å. *Biochem. Biophys. Res. Commun.* **2008**, *366*, 15−22.
(38) Gooden, D. M.; Schmidt, D. M. Z.; Pollock, J. A.; Kabadi, A. M.; McCafferty, D. G. Facile synthesis of substituted *trans*-2-arylcyclopropylamine inhibitors of the human histone demethylase LSD1 and monoamine oxidases A and B. *Bioorg. Med. Chem. Lett.* **2008**, *18*, 3047−3051.
(39) Lin, Y.; Wu, Y.; Li, J.; Dong, C.; Ye, X.; Chi, Y.-I.; Evers, B. M.; Zhou, B. P. The SNAG domain of Snail1 functions as a molecular hook for recruiting lysine-specific demethylase 1. *EMBO J.* **2010**, *29*, 1803−1816.
(40) Laurent, B.; Randrianarison-Huetz, V.; Frisan, E.; Andrieu-Soler, C.; Soler, E.; Fontenay, M.; Dusanter-Fourt, I.; Duménil, D. A short Gfi-1B isoform controls erythroid differentiation by recruiting the LSD1−CoREST complex through the dimethylation of its SNAG domain. *J. Cell Sci.* **2012**, *125*, 993−1002.
(41) Saleque, S.; Kim, J.; Rooke, H. M.; Orkin, S. H. Epigenetic Regulation of Hematopoietic Differentiation by Gfi-1 and Gfi-1b Is Mediated by the Cofactors CoREST and LSD1. *Mol. Cell* **2007**, *27*, 562−572.
(42) Friesner, R. A.; Banks, J. L.; Murphy, R. B.; Halgren, T. A.; Klicic, J. J.; Mainz, D. T.; Repasky, M. P.; Knoll, E. H.; Shelley, M.; Perry, J. K.; Shaw, D. E.; Francis, P.; Shenkin, P. S. Glide: A new approach for rapid, accurate docking and scoring. 1. Method and assessment of docking accuracy. *J. Med. Chem.* **2004**, *47*, 1739−1749.
(43) Xu, C.; Reichert, E. C.; Nakano, T.; Lohse, M.; Gardner, A. A.; Revelo, M. P.; Topham, M. K.; Stafforini, D. M. Deficiency of Phospholipase A2 Group 7 Decreases Intestinal Polyposis and Colon Tumorigenesis in ApcMin/+ Mice. *Cancer Res.* **2013**, *73*, 2806−2816.